Drier Bed Adsorption Predictive Model with Enhancement of Long Short-Term Memory and Particle Swarm Optimization

MarinaYusoff[1], Mohamad Taufik Mohd Sallehud-din[2], Nooritawati Md. Tahir[3], Wan Fairos Wan Yaacob[4], Nur Niswah Naslina Azid @ Maarof[5], Jasni Mohamad Zain[6], Putri Azmira R Azmi[7], Calvin Karunakumar[8]

Institute for Big Data Analytics and Artificial Intelligence (IBDAAI), Kompleks Al-Khawarizmi, Universiti Teknologi MARA (UiTM), 40450 Shah Alam, Selangor Darul Ehsan[1, 3, 4, 6, 7]

PETRONAS Research Sdn Bhd, Jln Ayer Hitam, Kawasan Institusi Bangi, 43000 Bandar Baru Bangi, Selangor[2]

College of Computing, Informatics and Media, Universiti Teknologi MARA Cawangan Kelantan, Kampus Kota Bharu, Lembah Sireh, Kota Bharu, 15050, Kelantan[5]

PETRONAS Research Sdn Bhd, Jln Ayer Hitam, Kawasan Institusi Bangi, 43000 Bandar Baru Bangi, Selangor[8]

***Abstract*—The drier bed adsorption processes remove moisture from gases and liquids by ensuring product quality, extending equipment lifespan, and enhancing safety in various applications. The longevity of adsorption beds is quantified by net loading capacity values that directly impact the effectiveness of the moisture removal process. Predictive modeling has emerged as a valuable tool to enhance drier bed adsorption systems. Despite the increasing significance of predictive modeling in enhancing the efficiency of drier bed adsorption processes, the existing methodologies frequently exhibit deficiencies in accuracy and flexibility, which are crucial for optimizing process performance. This research investigates the effectiveness of a hybrid approach combining Long Short-Term Memory and Particle Swarm Optimization (LSTM+PSO) as a proposed method to predict the net loading capacity of a drier bed. The train-test split ratios and rolling origin technique are explored to assess model performance. The findings reveal that LSTM+PSO with a 70:30 train-test split ratio outperform other methods with the lowest error. Bed 1 exhibits an RMSE of 1.31 and an MSE of 0.91, while Bed 2 archives RMSE and MSE values of 0.81 and 0.72, respectively and Bed 3 with an RMSE of 0.19 and an MSE of 0.13, followed by Bed 4 with an RMSE of 0.67 and an MSE of 0.36. Bed 5 exhibits an RMSE of 0.42 and an MSE of 0.34. Furthermore, this research compares LSTM+PSO with LSTM and conventional predictive methods: Support Vector Regression, Seasonal Autoregressive Integrated Moving Average with Exogenous Variables, and Random Forest.**

***Keywords*—Adsorption; Long Short-Term Memory; net loading capacity; Particle Swarm Optimization; prediction**

I. INTRODUCTION

Drying is used in various sectors, including agriculture, pharmaceuticals, energy, and other process industries, to transform liquid within a product into a solid [1], [2]. External energy, such as fossil fuel, generates high temperatures in a drying system's rotary bet, fluidized bed, spray, tray, impinging jet, and pulse combustion dryers [2]–[4]. This method involves drying wet goods at high temperatures [3], [4] to ensure the best possible performance. Drying techniques range from the sun to the oven, freezer, and microwave [3], [5]. Adsorption shows more promise than other drying methods when it comes to air drying [6].

The drier bed adsorption process is widely used across various industries [7], [8]. It is an essential parameter for estimating the remaining life of the drier bed and must coincide with the planned plant shutdown period. The overestimation of bed capacity will lead to unexpected moisture breakthroughs, resulting in production losses due to the drying out of equipment further down the line. In this research, Net Loading Capacity (NLC) measures the amount of moisture an adsorption bed can absorb before replacing or regenerating. An adsorption bed with a longer lifespan can extract more water before needing to be replaced or regenerated, which can maximize efficiency and save expenses. The challenge of accurately measuring dryer process system performance remains unaddressed despite its critical role in guaranteeing energy conservation, process dependability, and product quality [2, 4, and 9].

In recent years, Long Short-Term Memory (LSTM) neural networks are also known for their ability to model sequential data effectively, such as time series or text data. LSTM also has advanced potential for prediction modelling in various domains such as prediction of crude oil [10]–[12], financial [13], energy consumption [14]–[16], and medical [17]. Their capability to capture long-range dependencies and adapt to changing input patterns makes them a promising tool for modelling and predicting the dynamic behaviour of drier bed adsorption. However, performing well requires a large number of data and substantial computational resources. This makes them less suitable for small datasets due to overfitting. Furthermore, it can be sensitive to hyperparameter settings since finding the appropriate parameter can be time-consuming.

The optimization techniques are crucial in improving the prediction efficiency of the models. Particle Swarm Optimization (PSO) is a robust optimization algorithm inspired by birds flying for food, which has been widely applied to various optimization problems [18]. The combination and integration of PSO with LSTM aims to tackle the information

of particles to fine-tune the model parameters and optimize the prediction accuracy of the drier bed adsorption model of a small number of datasets.

The contributions of this paper are in the following:

1) A new particle representation is used for PSO implementation in an NLC drier bed performance-based molecular sieve.

2) A novel idea of combining LSTM with a new particle representation strategy of a PSO for predicting drier bed adsorption capacity, namely LSTM+PSO.

3) LSTM+PSO facilitates the analysis of temporal predictions, optimizing prediction models and improving prediction accuracy using a small number of adsorption bed life monitoring datasets.

4) A comparison analysis of LSTM+PSO with LSTM and traditional machine learning and statistical methods was performed.

The remainder of paper is organized by sections. Section II presents the related work. Section III delves into methodology detailing the architecture of the LSTM+PSO model and the optimization process. Section IV discusses the proposed solution, the model of LSTM+PSO performance with LSTM, SVR, and SARIMAX. Section V discusses the performance evaluation. Section VI gives the computational results. Section VII and Section VIII presents the discussion and conclusion respectively.

II. Related Work

Adsorption drying reduces the amount of water vapor in humid air by passing it through the solid adsorbent level of dehydration, which influences the selection of an appropriate adsorbent [6], [19]. Adsorbent bed dryers come in various configurations, including packed beds, coated channels, and annular coated tubes [20]. The bed's efficiency is affected by design parameters such as bed length and adsorbent mass [7]. The design of the drops must allow for high transfer rates while also being appropriately sized accommodating the allowable pressure drop [21]. Furthermore, the dryer should be stable over long periods of operation, have low toxicity, be corrosion resistant, and be cost-effective. Molecular sieves are an example of an adsorbent commonly used in natural gas plants [19]. The ability of water molecules to diffuse into the pores of the adsorbent limits the overall adsorption rate [6].

The advantages of adsorption drying include a low impact of temperature and pressure on the adsorption process, the use of simple equipment, reduced spatial demands, efficient humidification capabilities, the ability to use various heat sources for adsorbent regeneration, and cost-effective operation [6], [21]. The short adsorption-desorption cycles and low-temperature regeneration techniques are employed that can help achieve low operational costs [22]. Adsorption drying has several disadvantages, including increased heating costs, energy-intensive regeneration processes, and potential sorbent abrasion [9], [21]. Various approaches have been proposed to improve the limitations of estimating drying capacity to achieve optimal drying performance. These include the use of mathematical models, simulations of the drying apparatus, and machine learning techniques.

The use of a mathematical model for the drier indicates that it causes an increase in drying capacity to optimize the energy consumption of an amount of heat [23]. Furthermore, both the dryer efficiency and sustainability index demonstrate a significant reliance on the extent of heat recovery in the case of a spray dryer [24]. On the other hand, the significance of materials' drying behavior highlights limitations to enhance accuracy and reliability in adopting capillary active insulation materials [25]. The mathematical modeling for a multistage phosphate pellet roasting process offers the potential for significant energy savings [26]. However, there still needs to be more research on adsorption dryer beds, especially in the prediction of the NLC.

III. Material and Methods

This section explains the steps to address the predictive analytics challenge in drier bed adsorption, specifically in predicting NLC. The research framework begins with data acquisition, which involves data collection from five different beds: Bed 1, Bed 2, Bed 3, Bed 4, and Bed 5. Next, the data undergoes a pre-processing stage where unnecessary or irrelevant information, such as bad input and intf shut are eliminated to ensure data quality. Additionally, noisy data is filtered out to enhance the reliability of the dataset. The next step is featuring selection guided by correlation coefficients [27], which aims to identify the most relevant features for the predictive modeling task. The dataset is divided into training and testing subsets, setting the model development stage.

In the research model development phase, various methodologies comparing conventional methods such as LSTM, SVR, SARIMAX, and Random Forest are compared with the proposed LSTM+PSO. Fig. 1 provides a research framework. The data acquisition process involves the implementation of an automated procedure. In this research, computational analysis has been conducted focuses on the process within the drier beds for Bed 1, Bed 2, Bed 3, Bed 4, and Bed 5. The components that involve automatic breakthrough time identification, the identification and checking of the regeneration efficiency, and the identification regeneration cycle are all components of this step for each drier bed.

A. Data Pre-processing

Data pre-processing involves data extraction. The process of filtering historical data is handled by data extraction. A few steps in data processing are removing unnecessary data such as bad input, intf shut, and removing noisy data. Removing unnecessary data involves identifying and eliminating columns or variables within the dataset that either do not contribute valuable information or contain redundant information. During data processing, noisy data points are identified and filtered out.

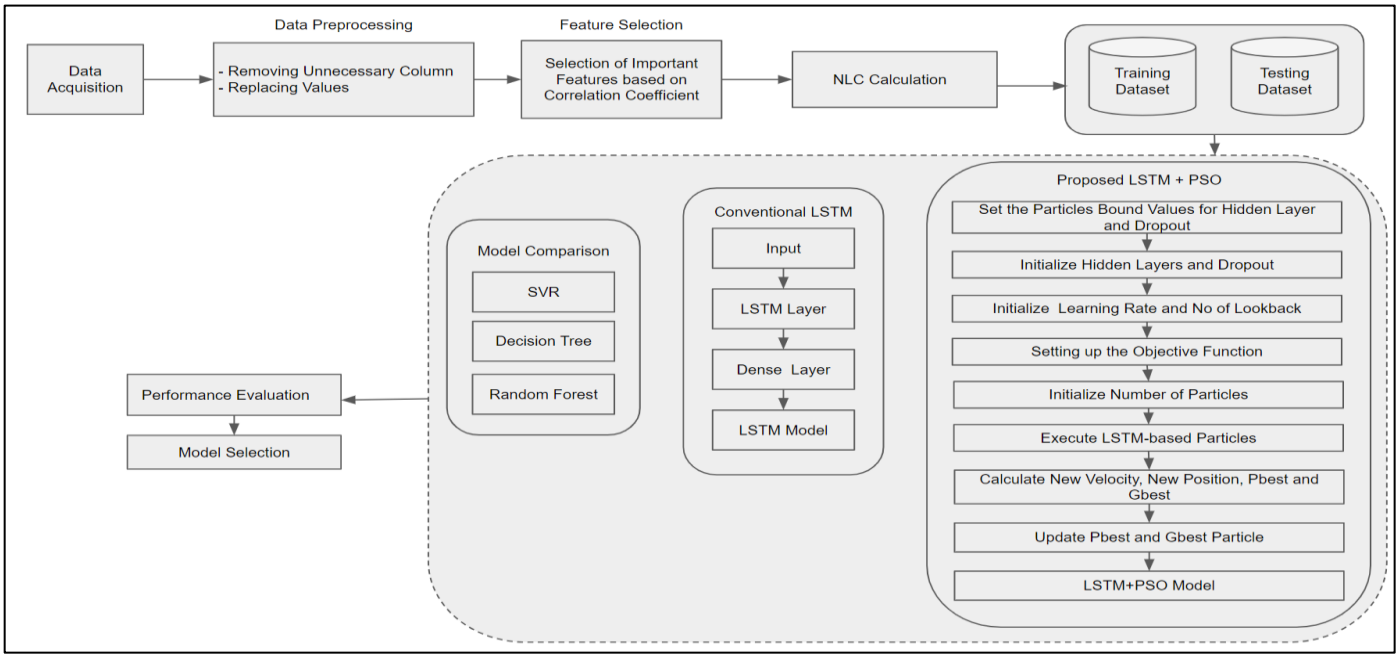

Fig. 1. Research framework.

B. Features Selection

The features are chosen based on their correlation with beds 1, 2, and 3 to identify the most relevant ones. The correlation can use two sets of correlation values: {0.1, 0.2, 0.3, 0.4, 0.5} and {-0.1, -0.2, -0.3, -0.4, -0.5}, calculated using the Pearson correlation coefficient. Eq. (1) presents the Pearson formulas for the correlation coefficient [27]. This coefficient ranges from -1 to 1. The coefficient value equal to -1 indicates a perfect negative correlation. Meanwhile, 1 indicates a perfect positive correlation. In addition, a zero value indicates no linear correlation between the variables.

$$r = \frac{\sum(x_i - \bar{x})(y_i - \bar{y})}{\sqrt{\sum(x_i - \bar{x})^2 \sum(y_i - \bar{y})^2}} \quad (1)$$

where, in these equations, r represents the correlation coefficient, x_i signifies the values of the variable of x in a sample, x denotes the mean (average) of the x variable values, y_i stands for the values of the y variable in a sample, and y represents the mean (average) of the y variable values.

C. Establishment of NLC Data

NLC data is crucial for predicting drier bed adsorption capacity. The values of NLC are drier bed. Historical datasets on drier bed adsorption were employed to build predictive and validation models. The calculation of NLC includes historical data features, regeneration processes, and breakthrough times for adsorption. Following the processes, the final datasets for each bed are less than 30. The challenge is to achieve good prediction accuracy with a small dataset.

IV. Proposed Solution

The proposed solution combines the strengths of LSTM and PSO for a more robust and practical approach for a small dataset. The LSTM network provides powerful sequence modeling capabilities. Meanwhile, PSO is used to fine-tune hyperparameters and optimize the performance of the LSTM model. This hybrid approach aims to utilize the strengths of both techniques to improve predictive accuracy and overall performance. Following are the details of the hybridization of LSTM+PSO.

A. Particle Representation

A real-value PSO implementation followed the initial PSO steps. This representation is new for PSO implementation, which supports a new strategy to be embedded in LSTM and a drier bed performance-based molecular sieve. Fig. 2 is the representation for the particle, $H = \{H_1, H_2, H_3, H_4, H_5 \ldots H_n\}$ and Dropout (DP). This representation defines the characteristics; include a number of layers including DP structure, within the optimization process in the search space.

H_1	H_2	DP

Fig. 2. Particle representation.

where, the parameters are defined as H_1 represents hidden layer 1 with a range of [0.80, 1.28], H_2 represents hidden layer 2 with a range of [0.80, 2.56], and DP with a range of [0.05, 0.50]. These parameter definitions specify the allowable values or ranges for each parameter within the optimization process of LSTM+PSO. Each particle component consists of layers and DP is randomly initiated in a population. A real value for all layers is initiated as in Eq. (2) and Eq. (3).

$$d = 2 * (np.random.rand(n, 1)) - 1 \quad (2)$$

$$d = rand(x, y) * z \quad (3)$$

Where, the variables are defined as *x*, *y*, and *z* represents indices used in layer calculations. *x* is a variable that takes values from the set {1, 2, 3, ..., *m*}. These indices are used for referencing through layers within a calculation. A particle update procedure was introduced, which is iteratively adjusted to identify the optimal model fit for the network. The dynamic range update is based on +8 or -8 for H_1 and H_2 values, and DP is an increased value of 0.01. Eq. (3) and Eq. (4) present the velocity and position formulas for the PSO, respectively.

$$V_{id\ (new)} = W * V_{id} + C_1 r_1 * \left(P_{best(id)}\right) - X_{id} + C_2 r_2 * \left(G_{best(id)} - X_{id}\right) \quad (4)$$

$$X_{id(new)} = X_{id} + V_{id\ (new)} \quad (5)$$

where, $V_{id(new)}$ represents the updated velocity, V_{id} stands for the current velocity, X_{id} denotes the current position, and $X_{id(new)}$ signifies the new position of a particle in a PSO. The parameters *W* represent the inertia weight, while C_1 and C_2 are the acceleration coefficients controlling the impact of personal and global best positions on particle movement. r_1 *and* r_2 are random functions or values used for stochastic behaviour. $P_{best(id)}$ represents the personal best position for a particle with the identifier id, and $G_{best(id)}$ signifies the global best position for the same particle identifier within the PSO algorithm.

B. LSTM+PSO Algorithm

A novel approach is a hybrid model that integrates the PSO algorithm and the LSTM; this model is intended to serve the oil and gas industry. Algorithm 1 provides an overview of the LSTM+PSO method. The LSTM+PSO optimize LSTM hyperparameters for prediction. The algorithm begins by initialization of particle values in Steps 1-2. This is vital for the PSO optimization process. Next, Steps 3-4 are initializing the particles with random values. Determine the number of past future data points in the LSTM model for Step 5.

Furthermore, Step 6 defines the objective function the PSO algorithm will optimize. This function measures the performance of the LSTM model on the given task. Initialize particles and iterations number in Steps 7-8. These steps specify the number of particles in the PSO optimization and set the maximum number of iterations for the PSO algorithm. Step 9 is loading the dataset that contains the selected features relevant to the task from the selected features. Step 10 is performing the feature scaling on the dataset to ensure that the data is within a consistent range, which is typically important for LSTM models. Split the dataset into training and testing sets for model evaluation and train the LSTM neural network with the initialized particles, which represent different configurations of the LSTM model in Steps 11-12.

Algorithm 1: LSTM+PSO	
1	Begin
2	Initialize particles
3	Initialize hidden layers and dropout-based particle values
4	Initialize learning rate
5	Set the number of lookbacks, number of future points
6	Setting up the objective function
7	Initialize particles number
8	Initialize iterations number
9	Load dataset from the selected features
10	Features scaling for LSTM fitting
11	Set the Train Test Split
12	Execute LSTM
13	Calculate Pbest and Gbest values for each particle
14	Do
15	For each particle
16	Calculate the new velocity value, $V_{(new)}$
17	Calculate new position, $D_{(new)}$
18	Calculate Pbest $_{(new)}$
19	Calculate Gbest $_{(new)}$
20	For each particle dimension
21	If current Pbest > current Gbest **Update new particle**
22	If current Pbest < current Gbest **Update new particle**
23	While (stopping condition is reached)
24	End

Moreover, evaluate the performance of each particle (LSTM configuration) using the objective function and determine the personal best (P_{best}) and global best (G_{best}). Step 14-Step 23 begins a loop. Iterate through each particle. The particle's velocity is updated based on its current Pbest and Gbest positions. The position of the particle is updated using the new velocity. Re-evaluate the performance of the particle with its new position and update Pbest if it improves in Step 18. Step 29 is to update the global best (G_{best}) if a particle of Pbest is better than the current Gbest. Iterate through each dimension of the particle by adjusting the particle dimension by subtracting and adding a particle change value in Step 20-Step 22. Continue the loop until a stopping condition is met, such as reaching a maximum number of iterations in Step 23. It marks the endpoint when the stopping condition is met or when the maximum number of iterations is reached.

In this research, LSTM is further enhanced by embedding the advantages of PSO. In this study, LSTM and PSO are combined. PSO can assist in finding an optimal solution, such as in obtaining a better architecture of LSTM. Fig. 1 demonstrates LSTM + PSO architecture. The main steps are similar to LSTM, which defines the input size, hidden layer, and output size. Input size corresponds to the number of input sequences or several features. The hidden layer size specifies the number of hidden layers, and the output size is set to 1, which indicates the number of items in the output predicts the NLC. The PSO elements are embedded for LSTM architecture determination.

V. PERFORMANCE EVALUATION

The next step is to train the data and define the epochs number using the train-test split and rolling origin. RMSE measures the average error between predicted and actual values, with lower values indicating better model accuracy. MAE represents the average absolute error, whereas lower values also suggest better model accuracy. Three types of

splitting are used: 70:30, 80:20, and 90:10, dividing between training and testing data. The model's performance will be evaluated by analyzing its ability to predict NLC.

The RMSE acceptance criteria [28]–[30] are categorized as follows: RMSE values falling within the range of ≤ 0.75 are considered very Good, while those between 0.75 and 1.0 are deemed Good. RMSE values ranging from 1.0 to 2.0 are labeled as satisfactory, and any RMSE exceeding 2.0 is categorized as unsatisfactory. These criteria provide a standardized assessment for evaluating the accuracy and quality of RMSE values in various applications or studies. RMSE equation is a mathematical expression used to quantify the average deviation between predicted values ($\hat{y}_i$) and actual values (y_i) within a regression model, as shown in Eq. (6).

$$RMSE = \sqrt{\sum_{i=1}^{n} \frac{(\hat{y}_i - y_i)^2}{n}} \quad (6)$$

The LSTM model also has the best performance based on the results of evaluation metrics MAE. The MAE acceptance criteria [31], [32], as referenced, are categorized as follows: MAE values between 0 and 3 are considered very good. Those falling within the range of 3 to 6 are labelled as good. MAE values between 6 and 9 are categorized as average, and if the MAE falls within the range of 9 to 12, it is referred to as variable data. Any MAE exceeding 12 is designated as higher variability. These criteria offer a standardized framework for assessing the quality and suitability of MAE values in different contexts or studies. The MAE equation is a mathematical formula used to quantify the variance between the prediction (y_i) and the real value (x_i) by dividing this variance by the square root of the number of data points in the observations (n), as shown in Eq. (7).

$$MAE = \frac{\sum_{i=1}^{n} |y_i - x_i|}{n} \quad (7)$$

VI. Computational Results

The computational results involve using root-mean-squared error (RMSE) and mean-squared error (MAE) metrics. These metrics are applied and compared to conventional methods using the setting of parameters to assess the effectiveness and suitability of the algorithm.

A. Parameter Setting

Table I outlines the parameter settings for the LSTM+PSO model. It specifies the values assigned to different parameters for training and evaluating the model. The train-test split parameter determines how the dataset is divided for training and testing with options of 90% training and 10% testing, 80% training and 20% testing, or 70% training and 30% testing.

The rolling origin parameter indicates the number of time steps considered when making predictions with 1, 2, or 3 options. The epoch parameter sets the number of times it is passed forward and backward through the LSTM network during training, which is set at 30. The learning rate parameter defines the step size at which the model adjusts its weights during optimization, set to 0.1. Finally, the batch size parameter determines the number of data points used in each iteration of the training process and is set to 256.

TABLE I. PARAMETER SETTING OF LSTM+PSO

Parameter	Value
Train-Test Split	90:10, 80:20, 70:30
Rolling Origin	1,2,3
Epoch	30
Learning Rate	0.1
Batch Size	256
Population	30

B. Computational Results using LSTM+PSO

The comparison computational results achieved through the LSTM+PSO approach are presented in Table II. The data was split using a 90:10, 80:20, and 70:30 ratio, which utilized a lookback of three for Bed 1, a lookback of two for Bed 2, and a lookback of four for Bed 3 for prediction. The LSTM+PSO that utilize a Train-Test Split ratio of 70:30 has demonstrated its effectiveness across Bed 1, Bed 2, Bed 3, Bed 4, and Bed 5, as indicated by both RMSE and MAE evaluations.

TABLE II. COMPUTATIONAL RESULT USING TRAIN-TEST SPLIT

Beds	Train-Test Split	RMSE	MAE
Bed 1	90:10	1.68	1.39
	80:20	1.53	1.16
	70:30	**1.31**	**0.91**
Bed 2	90:10	1.07	1.00
	80:20	0.97	0.90
	70:30	**0.81**	**0.72**
Bed 3	90:10	0.28	0.21
	80:20	0.21	0.15
	70:30	**0.19**	**0.13**
Bed 4	90:10	0.71	0.54
	80:20	0.70	0.56
	70:30	**0.67**	**0.36**
Bed 5	90:10	0.46	0.38
	80:20	0.45	0.37
	70:30	**0.42**	**0.34**

For Bed 1, an RMSE score of 1.31 falls within the satisfactory range, indicating that the predictive model provides reasonably accurate results for this bed. Furthermore, the MAE value of 0.91 is categorized as very good, signifying that the model's prediction closely aligns with the actual values. It demonstrates a high level of accuracy as compared to other percentages of Train-Test Split. Moving on to Bed 2, the RMSE score of 0.81 is good, implying that the model delivers accurate predictions with a relatively low margin of error.

Similarly, the MAE value of 0.72 is labeled as very good, indicating that the model's performance is highly accurate for Bed 2. In addition, for Bed 3, an RMSE score of 0.19 is

considered satisfactory. This suggests that the accuracy of the model is acceptable. It is worth noting that the MAE value of 0.13 is once again classified as very good by underscoring the model's capability to make highly accurate predictions for Bed 3. Furthermore, in the case of Bed 4, the RMSE score of 0.67 is categorized as good. This indicates that the predictive model provides accurate predictions with a relatively small margin of error for Bed 4. Additionally, the MAE value of 0.36 is labeled as very good and highlights that the model's performance is highly accurate when predicting outcomes for Bed 4. Lastly, for Bed 5, the RMSE shows a good value, which is 0.42, along with the MAE obtained of about 0.34, which indicates good performance to the predictive model.

Table III presents an analysis of performance metrics, specifically RMSE and MAE, for various bed types (Bed 1, Bed 2, Bed 3) across rolling origin values of 1, 2, and 3. The LSTM+PSO approach applied rolling origin has consistently proven its effectiveness in predicting outcomes for Bed 1 until bed 3, as evidenced by the RMSE and MAE assessments. Notably, for Bed 1, the RMSE of 1.78 falls within the satisfactory range, while the MAE of 1.62 is categorized as very good. Similarly, for Bed 2, the RMSE of 0.82 is deemed suitable, and the MAE of 1.08 is labeled very good. For Bed 3, the RMSE of 0.70 is considered satisfactory, and the MAE of 0.14 is classified as very good.

TABLE III. COMPUTATIONAL RESULT USING ROLLING ORIGINS

Types of Beds	Rolling Origin	RMSE	MAE
Bed 1	**1**	**1.78**	**1.62**
	2	2.00	1.79
	3	2.46	2.19
Bed 2	**1**	**0.82**	**1.08**
	2	0.93	1.18
	3	1.17	1.28
Bed 3	**1**	**0.70**	**0.14**
	2	1.21	0.80
	3	1.42	0.38

C. Computational Results with LSTM and Conventional Methods

The comparison experimental results of conventional methods of LSTM, SVR, SARIMAX, Random Forest (RF), and LSTM+PSO are shown in Table IV. The choice of parameter settings for the split percentage of 70:30 is similar to the LSTM+PSO approach. A lower RMSE and MAE suggest superior predictive performance and indicate that the model's prediction is closer and aligned to the actual values.

In the case of Bed 1, the SARIMAX and RF models showed better results than the LSTM, SVR, and LSTM+PSO models. It was evident through their lower values of RMSE and MAE. Moreover, it can be observed that LSTM+PSO exhibits the highest predictive accuracy in terms of both RMSE and MAE metrics for Bed 2, Bed 3, Bed 4, and Bed 5. Regardless of SARIMAX and RF demonstrating lower values of RMSE and MAE, they are not suitable for forecasting due to their inability to accommodate the lookback value, resulting in unviable forecast points.

TABLE IV. COMPUTATIONAL RESULT WITH CONVENTIONAL METHOD

Types of Beds	Metrics	LSTM	SVR	SARIMAX	RF	LSTM+PSO
Bed 1	RMSE	1.45	2.81	1.18	1.10	**1.31**
	MAE	1.33	2.79	0.76	0.99	**0.91**
Bed 2	RMSE	0.69	1.08	4.68	1.12	**0.61**
	MAE	0.53	1.03	3.59	1.04	**0.45**
Bed 3	RMSE	0.55	3.93	3.96	1.26	**0.19**
	MAE	0.46	3.71	3.50	1.21	**0.13**
Bed 4	RMSE	0.83	1.36	4.68	1.36	**0.67**
	MAE	0.55	0.99	3.59	1.27	**0.36**
Bed 5	RMSE	0.49	3.94	2.69	1.08	**0.42**
	MAE	0.32	3.71	2.18	0.85	**0.34**

VII. DISCUSSIONS

LSTM+PSO model, especially when utilizing a train-test split ratio of 70:30, is highly effective in predicting results for a difference of beds, namely, Bed 1, Bed 2, Bed 3, Bed 4, and Bed 5. The model can perform well. The prediction result of LSTM+PSO using rolling origin highlights the reliability of the LSTM+PSO approach in achieving precise predictions across different bed types. However, it is worth noting that the rolling origin method, while promising, may utilize only some of the dataset as effectively as a fixed train-test split of 70:30, as it involves random cross-validation that may exclude some data observations [33].

The most notable outcome of this study is that the LSTM+PSO model outperformed other models such as LSTM, SVR, Random Forest, and SARIMAX, as evident by lower RMSE and MAE values. It highlights the effectiveness of the LSTM+PSO model in making predictions on the dataset. The LSTM+PSO can be advantageous in terms of exploration, exploitation [34], [35], stochastic search, optimal capability, and the ability to handle global and local optima [36], [37]. PSO is known for its ability to explore the search space effectively. When combined with LSTM, which tends to converge quickly to local optima, PSO helps explore different regions of the parameter space, potentially leading to better global solutions.

While LSTM is good at fine-tuning, the PSO algorithm attracts other particles toward the region. The stochastic behaviour helps to escape local optima, which can be especially beneficial when combined with LSTM, which tends to be deterministic [38]–[40]. LSTM+PSO can harness the optimal capability of PSO to find the best set of hyperparameters of weights for the LSTM that can lead to improved overall model performance. It also allows for a more robust optimization process to improve model performance, especially in complex and high-dimensional search spaces. Thus, PSO is designed to handle both global and local optima that complement LSTM's ability to fine-tune models to local patterns in small datasets.

VIII. CONCLUSION

The LSTM+PSO method is proposed for NLC prediction of a drier bed, which can assist manual moisture adsorption capacity test. LSTM+PSO utilized a new particle

representation to obtain a robust model for predicting outcomes for different bed types. Compared with LSTM, SVR RF, and SARIMAX, the proposed LSTM+PSO performs better, achieving significantly lower RMSE and MAE values for a small dataset. Additionally, a new particle representation LSTM+PSO, an efficient model, is achieved for predicting outcomes on different bed types. This achievement provides significant possibilities for improving future investigations within this domain. In future research efforts, it is suggested to incorporate additional data from alternative sources, such as other beds, together with experimental data collected over a period. This approach will facilitate the analysis of temporal predictions, allowing for the refinement of prediction models and the enhancement of prediction accuracy. Additional techniques, such as cuckoo search and firefly algorithm will be employed in future research to reduce the error and obtain an optimal solution.

ACKNOWLEDGMENT

The authors would like to acknowledge the PETRONAS Academia Collaboration Grant, Institute for Big Data Analytics and Artificial Intelligence (IBDAAI), and Universiti Teknologi MARA for the financial support provided to this research project.

REFERENCES

[1] S. Banooni, E. Hajidavalloo, and M. Dorfeshan, "Experimental and numerical study of the effects of pre-drying of S-PVC using a pneumatic dryer," Powder Technol, vol. 338, pp. 220–232, 2018, doi: 10.1016/j.powtec.2018.06.027.

[2] B. Lan, P. Zhao, J. Xu, B. Zhao, M. Zhai, and J. Wang, "CFD-DEM-IBM simulation of particle drying processes in gas-fluidized beds," Chem Eng Sci, vol. 255, 2022, doi: 10.1016/j.ces.2022.117653.

[3] M. R. Nukulwar and V. B. Tungikar, "Recent development of the solar dryer integrated with thermal energy storage and auxiliary units," Thermal Science and Engineering Progress, vol. 29. Elsevier Ltd, 2022. doi: 10.1016/j.tsep.2021.101192.

[4] W. Su, D. Ma, Z. Lu, W. Jiang, F. Wang, and Z. Xiaosong, "A novel absorption-based enclosed heat pump dryer with combining liquid desiccant dehumidification and mechanical vapor recompression: Case study and performance evaluation," Case Studies in Thermal Engineering, vol. 35, 2022, doi: 10.1016/j.csite.2022.102091.

[5] M. Mohseni, A. Kolomijtschuk, B. Peters, and M. Demoulling, "Biomass drying in a vibrating fluidized bed dryer with a Lagrangian-Eulerian approach," International Journal of Thermal Sciences, vol. 138, pp. 219–234, 2019, doi: 10.1016/j.ijthermalsci.2018.12.038.

[6] M. Djaeni, D. Q. A'yuni, M. Alhanif, C. L. Hii, and A. C. Kumoro, "Air dehumidification with advance adsorptive materials for food drying: A critical assessment for future prospective," Drying Technology, vol. 39, no. 11, pp. 1648–1666, 2021, doi: 10.1080/07373937.2021.1885042.

[7] B. El Fil and S. Garimella, "Energy-efficient gas-fired tumble dryer with adsorption thermal storage," Energy, 2022, doi: 10.1016/j.energy.2021.121708.

[8] A. M. Nandhu Lal et al., "A comparison of the Refrigerated Adsorption Drying of Daucus carota with fluidized bed drying," LWT, 2022, doi: 10.1016/j.lwt.2021.112749.

[9] H. Daghooghi-Mobarakeh, M. Miner, L. Wang, R. Wang, and P. E. Phelan, "Application of ultrasound in regeneration of silica gel for industrial gas drying processes," Drying Technology, vol. 40, no. 11, pp. 2251–2259, 2022, doi: 10.1080/07373937.2021.1929296.

[10] K. Zhang and M. Hong, "Forecasting crude oil price using LSTM neural networks," Data Science in Finance and Economics, 2022, doi: 10.3934/dsfe.2022008.

[11] A. Manowska and A. Bluszcz, "Forecasting Crude Oil Consumption in Poland Based on LSTM Recurrent Neural Network," Energies (Basel), 2022, doi: 10.3390/en15134885.

[12] R. H. Assaad and S. Fayek, "Predicting the Price of Crude Oil and its Fluctuations Using Computational Econometrics: Deep Learning, LSTM, and Convolutional Neural Networks," Econometric Research in Finance, 2021, doi: 10.2478/erfin-2021-0006.

[13] S. Siami-Namini, N. Tavakoli, and A. S. Namin, "A Comparative Analysis of Forecasting Financial Time Series Using ARIMA, LSTM, and BiLSTM," 2019, [Online]. Available: http://arxiv.org/abs/1911.09512

[14] K. Yan, W. Li, Z. Ji, M. Qi, and Y. Du, "A Hybrid LSTM Neural Network for Energy Consumption Forecasting of Individual Households," IEEE Access, 2019, doi: 10.1109/ACCESS.2019.2949065.

[15] D. Durand, J. Aguilar, and M. D. R-Moreno, "An Analysis of the Energy Consumption Forecasting Problem in Smart Buildings Using LSTM," Sustainability (Switzerland), 2022, doi: 10.3390/su142013358.

[16] A. A. Ewees, M. A. A. Al-qaness, L. Abualigah, and M. A. Elaziz, "HBO-LSTM: Optimized long short term memory with heap-based optimizer for wind power forecasting," Energy Convers Manag, vol. 268, 2022, doi: 10.1016/j.enconman.2022.116022.

[17] S. U. M. Rao, K. V. Rao, and P. V. G. D. P. Reddy, "Medical Big Data Analysis using LSTM based Co-Learning Model with Whale Optimization Approach," International Journal of Intelligent Engineering and Systems, vol. 15, no. 4, pp. 627 – 636–627 – 636, 2022, doi: 10.22266/ijies2022.0831.56.

[18] Y. Choi et al., "Time-series clustering approach for training data selection of a data-driven predictive model: Application to an industrial bio 2,3-butanediol distillation process," Comput Chem Eng, vol. 161, 2022, doi: 10.1016/j.compchemeng.2022.107758.

[19] R. Gomes Santiago et al., "Investigation of premature aging of zeolites used in the drying of gas streams," Chem Eng Commun, vol. 206, no. 11, pp. 1378–1385, 2019, doi: 10.1080/00986445.2018.1533468.

[20] B. El Fil and S. Garimella, "Heat recovery, adsorption thermal storage, and heat pumping to augment gas-fired tumble dryer efficiency," J Energy Storage, 2022, doi: 10.1016/j.est.2021.103949.

[21] L. A. Nikolaeva, R. Zainullina, and A. K. Al'-Okbi, "Adsorption Drying of Natural Gas by Carbonate Sludge," Chemical and Petroleum Engineering, vol. 54, no. 11–12, pp. 919–925, 2019, doi: 10.1007/s10556-019-00572-2.

[22] M. R. Petryk, A. Khimich, M. M. Petryk, and J. Fraissard, "Experimental and computer simulation studies of dehydration on microporous adsorbent of natural gas used as motor fuel," Fuel, vol. 239, pp. 1324–1330, 2019, doi: 10.1016/j.fuel.2018.10.134.

[23] T. Mołczan and P. Cyklis, "Mathematical Model of Air Dryer Heat Pump Exchangers," Energies (Basel), 2022, doi: 10.3390/en15197092.

[24] S. K. Patel and M. H. Bade, "Energy analysis and heat recovery opportunities in spray dryers applied for effluent management," Energy Convers Manag, 2019, doi: 10.1016/j.enconman.2019.02.065.

[25] A. Rieser, D. Herrera-Avellanosa, E. Leonardi, M. Larcher, and R. Pfluger, "Experimental measurement of material's drying coefficient for internal insulation: New approaches for laboratory testing," in IOP Conference Series: Earth and Environmental Science, 2021. doi: 10.1088/1755-1315/863/1/012048.

[26] V. Meshalkin, V. Bobkov, M. Dli, and V. Dovì, "Optimization of energy and resource efficiency in a multistage drying process of phosphate pellets," Energies (Basel), 2019, doi: 10.3390/en12173376.

[27] L. Xu, Y. Wang, L. Mo, Y. Tang, F. Wang, and C. Li, "The research progress and prospect of data mining methods on corrosion prediction of oil and gas pipelines," Eng Fail Anal, vol. 144, p. 106951, 2023, doi: https://doi.org/10.1016/j.engfailanal.2022.106951.

[28] A. S. B. Karno, "Prediksi Data Time Series Saham Bank BRI Dengan Mesin Belajar LSTM (Long ShortTerm Memory)," Journal of Informatic and Information Security, 2020, doi: 10.31599/jiforty.v1i1.133.

[29] E. Kristiani, H. Lin, J. R. Lin, Y. H. Chuang, C. Y. Huang, and C. T. Yang, "Short-Term Prediction of PM2.5 Using LSTM Deep Learning Methods," Sustainability (Switzerland), 2022, doi: 10.3390/su14042068.

[30] Y. T. Tsan, D. Y. Chen, P. Y. Liu, E. Kristiani, K. L. P. Nguyen, and C. T. Yang, "The Prediction of Influenza-like Illness and Respiratory Disease Using LSTM and ARIMA," Int J Environ Res Public Health, 2022, doi: 10.3390/ijerph19031858.

[31] S. H. Bhatti, F. W. Khan, M. Irfan, and M. A. Raza, "An effective approach towards efficient estimation of general linear model in case of heteroscedastic errors," Commun Stat Simul Comput, 2023, doi: 10.1080/03610918.2020.1856874.

[32] İ. Y. Genç, "Prediction of storage time in different seafood based on color values with artificial neural network modeling," J Food Sci Technol, 2022, doi: 10.1007/s13197-021-05269-0.

[33] J. A. Fiorucci and F. Louzada, "GROEC: Combination method via Generalized Rolling Origin Evaluation," Int J Forecast, vol. 36, no. 1, pp. 105–109, 2020, doi: https://doi.org/10.1016/j.ijforecast.2019.04.013.

[34] J. H. Elrefaei, A. H. Madian, A. Yahya, M. K. Shaat, and R. M. Fikry, "A Modified Particle Swarm Optimization Approach for Latency of Wireless Sensor Networks," International Journal of Advanced Computer Science and Applications, vol. 12, no. 6, pp. 676–685, 2021, doi: 10.14569/IJACSA.2021.0120679.

[35] M. Elveny, M. K. M. Nasution, and R. B. Y. Syah, "A Hybrid Metaheuristic Model for Efficient Analytical Business Prediction," International Journal of Advanced Computer Science and Applications, vol. 14, no. 8, pp. 433–440, 2023, doi: 10.14569/IJACSA.2023.0140848.

[36] G. Dominico and R. S. Parpinelli, "Multiple global optima location using differential evolution, clustering, and local search," Appl Soft Comput, vol. 108, p. 107448, 2021, doi: https://doi.org/10.1016/j.asoc.2021.107448.

[37] Z. Meng, Y. Zhong, G. Mao, and Y. Liang, "PSO-sono: A novel PSO variant for single-objective numerical optimization," Inf Sci (N Y), vol. 586, pp. 176–191, 2022, doi: https://doi.org/10.1016/j.ins.2021.11.076.

[38] G. Tang, J. Sheng, D. Wang, and S. Men, "Continuous Estimation of Human Upper Limb Joint Angles by Using PSO-LSTM Model," IEEE Access, 2021, doi: 10.1109/ACCESS.2020.3047828.

[39] X. Gao, Y. Guo, D. A. Hanson, Z. Liu, M. Wang, and T. Zan, "Thermal error prediction of ball screws based on PSO-LSTM," International Journal of Advanced Manufacturing Technology, 2021, doi: 10.1007/s00170-021-07560-y.

[40] Q. Li, X. Chai, C. Zhang, X. Wang, and W. Ma, "Prediction Model of Ischemic Stroke Recurrence Using PSO-LSTM in Mobile Medical Monitoring System," Comput Intell Neurosci, 2022, doi: 10.1155/2022/8936103.